American Mineralogist, Volume 83, pages 638–651, 1998

Boralsilite ($Al_{16}B_6Si_2O_{37}$): A new mineral related to sillimanite from pegmatites in granulite-facies rocks

EDWARD S. GREW,[1,*] JAMES J. MCGEE,[2] MARTIN G. YATES,[1] DONALD R. PEACOR,[3] ROLAND C. ROUSE,[3] JOEP P.P. HUIJSMANS,[4] CHARLES K. SHEARER,[5] MICHAEL WIEDENBECK,[6] DOUGLAS E. THOST,[7] AND SHU-CHUN SU[8]

[1]Department of Geological Sciences, University of Maine, Orono, Maine 04469, U.S.A.
[2]Department of Geological Sciences, University of South Carolina, Columbia, South Carolina 29208, U.S.A.
[3]Department of Geological Sciences, University of Michigan, Ann Arbor, Michigan 48109, U.S.A.
[4]Netherlands Energy Research Foundation, P.O. Box 1, NL 1755 ZG Petten, The Netherlands
[5]Institute of Meteoritics, University of New Mexico, Albuquerque, New Mexico 87131, U.S.A.
[6]Advanced Materials Laboratory, University of New Mexico, Albuquerque, New Mexico 87106, U.S.A.
[7]Australian Geological Survey Organization, G.P.O. Box 378, Canberra A.C.T., Australia
[8]Hercules Research Center, 500 Hercules Road, Wilmington, Delaware 19808, U.S.A.

ABSTRACT

Boralsilite, the first natural anhydrous Al-B-silicate, is a high-temperature phase in pegmatites cutting granulite-facies metapelitic rocks at Larsemann Hills, Prydz Bay, east Antarctica (type locality) and Almgjotheii in the contact aureole of the Rogaland Intrusive Complex, southwestern Norway. Stable assemblages include: (1) quartz-potassium feldspar-boralsilite-schorl/dravite (Larsemann Hills); (2) potassium feldspar-plagioclase(An_{22})-boralsilite-werdingite-dumortierite-grandidierite (Almgjotheii); (3) quartz-potassium feldspar-boralsilite-dumortierite-andalusite ± sillimanite (Almgjotheii). Boralsilite is estimated to have formed between 600 and 750 °C and 3–5 kbar at conditions where $P_{H_2O} < P_{tot}$. The name is from the composition, *bor*on, *al*uminum, and *sil*icon. Representative electron and ion microprobe (SIMS) analyses of Larsemann Hills are: SiO_2 10.05 [12.67]; Al_2O_3 71.23 [69.15]; FeO 0.48 [1.10]; MgO below detection [0.23]; BeO 0.004 [0.094]; B_2O_3 19.63 [18.11] wt%, totals 101.39 [101.35] wt% where the numbers in brackets were determined from Almgjotheii material. However, the SIMS B_2O_3 values appear to be systematically too high; boron contents calculated assuming B + Si = 8 and O = 37 atoms per formula unit (apfu) yield B_2O_3 18.53 wt% corresponding to $Fe_{0.08}Al_{15.98}B_{6.09}Si_{1.91}O_{37}$ ideally $Al_{16}B_6Si_2O_{37}$ for Larsemann Hills. The analogous composition of $Mg_{0.07}Fe_{0.18}Al_{15.66}Be_{0.04}B_{5.565}Si_{2.435}O_{37}$ for Almgjotheii appears to result from solid solution of boralsilite with sillimanite (or $Al_8B_2Si_2O_{19}$) and subordinate werdingite. Boralsilite forms prisms up to 2 mm long $\|b$ and 0.25 mm across and is commonly euhedral in cross section. It is colorless and prismatic cleavage is fair. Optically, it is biaxial (+); at λ = 589 nm, the Larsemann Hills material has α = 1.629(1), β = 1.640(1), γ = 1.654(1), $2V_{meas}$ = 81.8 (6), $r > v$ extremely weak, and $\gamma\|b$. It is monoclinic, space group $C2/m$ with lattice parameters for Larsemann Hills of a = 14.767(1), b= 5.574(1), c = 15.079 (1) Å, β = 91.96(1)°, V = 1240.4 (2) Å^3, Z = 2, and D_{calc} = 3.07 g/cm^3.

INTRODUCTION

The new mineral boralsilite is the first anhydrous Al-B-silicate to be discovered in nature. This high-temperature phase occurs in two pegmatites cutting granulite-facies metapelitic rocks, one each at two localities: (1) Stornes Peninsula, Larsemann Hills, Prydz Bay, east Antarctica (69°24′ S, 76°07′ E), and (2) Almgjotheii in the aureole of the Rogaland intrusive complex, southwestern Norway (58°33′ N, 6°31′ E), upgrade from the hypersthene-in isograd (Tobi et al. 1985). Boralsilite is also the first reported naturally occurring compound related to synthetic, ternary Al-B-Si compounds orthorhombic in symmetry and having structural affinities to sillimanite and mullite ("boron-mullites," Werding and Schreyer 1984, 1996). Subsequently, Werding and Schreyer (personal communication) succeeded in hydrothermally synthesizing boralsilite at 1–4 kbar and 700–800 °C.

The discovery of boralsilite began with the description and analysis of Huijsmans (1981) and Huijsmans et al. (1982) of an unknown columnar mineral from the Almgjotheii pegmatite. Subsequent study showed the unknown mineral to consist of two distinct minerals (Grew 1996): werdingite, from which Huijsmans's (1981) anal-

* E-mail: esgrew@maine.maine.edu

0003–004X/98/0506–0638$05.00

TABLE 1. Minerals in the studied thin sections

Locality	Larsemann Hills		Almgjotheii, Norway			
Specimen	8812905		HE138B			
Section no.	1–2	3–6	1	2	3	4
Quartz (Qtz)	X	X	X	X	X	X
Potassium feldspar (Kfs)	X	X	X	X	X	X
Plagioclase (Pl)	T	—	T	—	T	X
Muscovite, secondary (Ms)	T	T	T	T	T	T
Chlorite, secondary	—	—	—	—	T	T
Sillimanite (Sil)	—	—	T	—	?	T
Andalusite (And)	—	—	T	T	T	X
Tourmaline (Tur)	X	X	X	X	X	X
Grandidierite (Gdd)	—	—	X	X	X	X
Dumortierite (Dum)						
Rose, high-Ti	—	—	—	T	X	X
Blue to purple, low-Ti	—	—	T	T	T	T
Werdingite (Wrd)	—	—	T	X	X	—
Boralsilite (Bor)	—	X	X	X	X	T
Hercynite	—	—	T	—	T	T
Corundum (Crn)	—	—	T	T	T	T
Diaspore, secondary	—	T	—	—	—	—
Rutile	T	T	—	—	—	—
Leucoxene	—	—	T	—	T	—
Wolframite	—	—	—	—	—	T
Pyrite	—	T	—	—	—	—
Apatite	T	T	T	—	—	—
Zircon	T	—	T	—	—	T
Xenotime	T	T	T	—	—	—
Monazite	?	—	T	—	T	—

Note: X = major constituent, T = trace constituent (in a given section). Mineral abbreviations follow Kretz (1983) and Grew (1996).

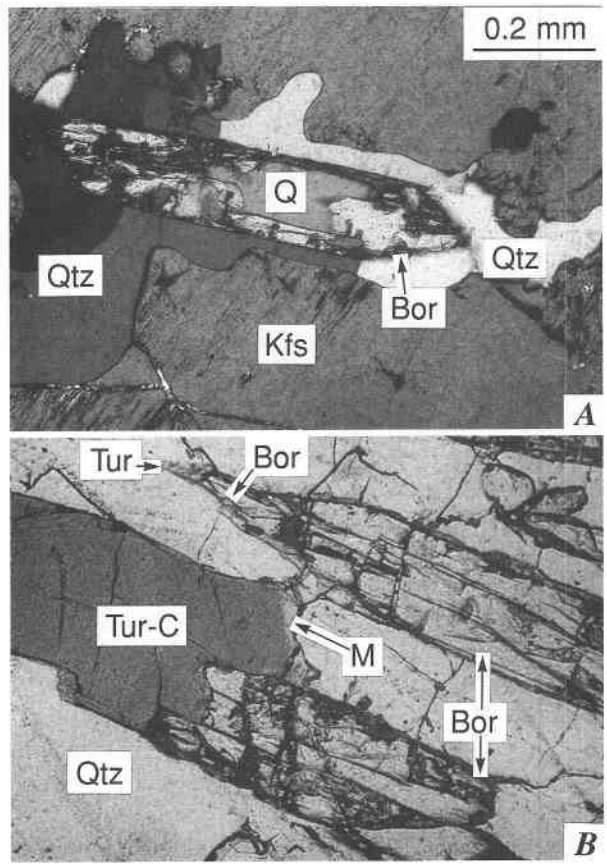

FIGURE 1. Photomicrographs of specimen no. 8812905, Larsemann Hills, east Antarctica. (**A**) A skeletal boralsilite prism (Bor) in quartz (Qtz, Q) separating it from potassium feldspar (Kfs). Crossed nicols. (**B**) Boralsilite surrounded by blue tourmaline (Tur) in quartz. M indicates the analyzed pale margin of the tourmaline; the core area is darker, Tur-C (see Table 7, col. 2–3, respectively). Plane light.

yses were obtained (Grew et al. 1998), and a new phase (described in this paper) with optical properties and composition distinct from those of werdingite. The Almgjotheii material was intractable for X-ray study. Characterization of the new mineral was realized after the serendipitous discovery that a sillimanite-like mineral in a tourmaline-quartz intergrowth collected by D.E. Thost in 1988 from the Larsemann Hills was identical to the second mineral in Huijsmans's specimen. This sample was amenable to X-ray study, and thus Larsemann Hills is designated the type locality.

The name is from the composition, *bor*on, *al*uminum, and *sil*icon. The new mineral and the name have been approved by the Commission on New Minerals and Mineral Names of the IMA. Holotype material is preserved in the National Museum of Natural History, Smithsonian Institution as NMNH 171403 and the Almgjotheii specimen as NMNH 171404.

PETROGRAPHIC DESCRIPTION

Larsemann Hills, Antarctica

Boralsilite has been found in a single specimen: D. Thost's no. 8812905 from the Stornes Peninsula (Table 1). This specimen is a tourmaline-quartz intergrowth consisting of black tourmaline grains up to 1 cm long and gray quartz. Feldspar grains (to 1 cm) are pinkish and scattered through the intergrowth. Boralsilite forms a single patch of fibrous aggregates of fine prisms in a quartz-rich part of the specimen. In thin section, the prisms are typically 0.05–0.3 mm wide, up to 2 mm long $\|b$, and commonly lie parallel to one another. The prisms occur either in open clusters or tight bundles up to 1 cm long. Some have a euhedral cross section (rhombic or pseudohexagonal). Boralsilite is, to varying degrees, replaced by diaspore (confirmed by electron microprobe analysis) and by a low-birefringence material, which could be kaolinite, the lines of which were noted in an X-ray powder pattern. Boralsilite occurs mostly in quartz, but a few prisms are found in potassium feldspar. The latter prisms are either isolated from potassium feldspar by a quartz selvage (Fig. 1A) or entirely pseudomorphed by the low-birefringence material. Nonetheless, local contacts of the pseudomorphs with potassium feldspar imply the former coexistence of potassium feldspar with boralsilite. No plagioclase was found near boralsilite. Zoned blue tourmaline locally appears between or around boralsilite prisms (Fig. 1B). This tourmaline is distinct in color and composition from the dominant and earliest-formed tourmaline in the intergrowth, which is black in hand specimen, moderate to dark olive (ω) in thin section, and gen-

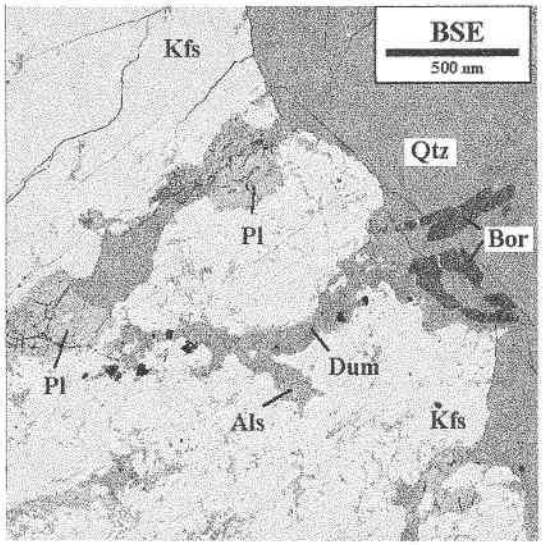

FIGURE 2. Backscattered electron image of boralsilite (Bor) in quartz (Qtz) near potassium feldspar (Kfs) cut by quartz vein. Several dumortierite grains (e.g., Dum) and one Al_2SiO_5 grain (Als) are present in the quartz, but cannot be distinguished in this image. Analyses of boralsilite and dumortierite are listed in Tables 5 (columns 6 and 7) and 6 (column 1). Plagioclase (Pl). Specimen no. HE138B3, Almgjotheii, Norway.

erally not strongly zoned. A later zoned olive-colored tourmaline is mostly lighter colored than the dominant variety. Euhedral grains of later formed, highly zoned, olive and blue tourmaline are also present.

Almgjotheii, Rogaland, Norway

The unknown mineral described by Huijsmans (1981) was found in one large specimen (HE138) that he collected in 1979 (Grew et al. 1998). Boralsilite has been positively identified in only one of the six fragments of this large specimen (HE138B, Table 1). Boralsilite occurs in the following textures in increasing order of abundance: (1) in parallel growth with grandidierite; (2) in prisms typically 0.05–0.2 mm wide, some of which have a rhombic cross section; such prisms are commonly aggregated (Fig. 2); (3) in bundles and sheaves of intergrown boralsilite and werdingite prisms, which are nearly parallel or diverge somewhat (Fig. 3 in Grew et al. 1998). Many of the individual prisms in these bundles are ladderlike ("scalariform") intergrowths of werdingite and boralsilite in which lamellae are oriented perpendicular to the prism direction (Fig. 3). These intergrowths presumably resulted from exsolution of werdingite-boralsilite solid solutions, but it is possible that they are a growth feature. In section HE138B4, boralsilite was observed only in backscattered electron (BSE) images of quartz microveinlets in potassium feldspar.

Boralsilite is most closely associated with quartz, potassium feldspar, plagioclase, dumortierite, grandidierite, tourmaline, andalusite, and possibly sillimanite (Table 1). In addition to its being in parallel growth with coarse

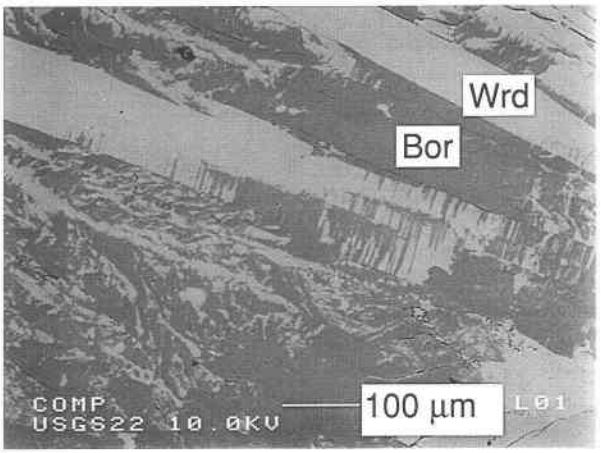

FIGURE 3. Backscattered electron image of boralsilite (black)-werdingite (gray) intergrowth, illustrating ladderlike ("scalariform") intergrowth. Specimen no. HE138B2.

grandidierite (>1 cm long), boralsilite is found mixed with finer-grained grandidierite and werdingite in a plagioclase (An_{22} in one spot) aggregate in HE138B1 (Fig. 4). The finer-grained (<2 mm) blue to purple variety of dumortierite is closely associated with boralsilite (e.g., Figs. 2 and 4); the rose variety, which appears to have formed earlier (Grew et al. 1998), forms grains and aggregates up to 6 mm across, commonly highly twinned. Tourmaline forms seams penetrating boralsilite-werdingite intergrowths and narrow blue overgrowths around

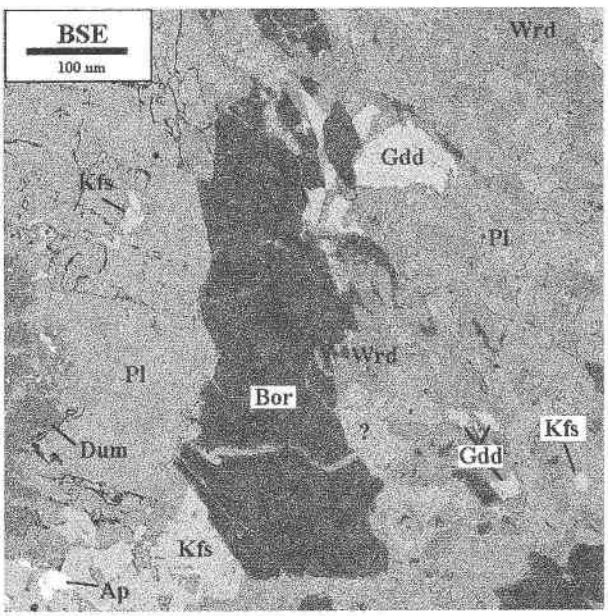

FIGURE 4. Backscattered electron image of boralsilite (black), werdingite (Wrd), grandidierite (Gdd), dumortierite (mass at left edge of image, Dum), potassium feldspar (Kfs) in plagioclase (Pl). Ap = apatite; ? = a secondary phyllosilicate. Specimen no. HE138B1.

TABLE 2. Optical properties of sillimanite-like minerals

	2V	α	δ	Twins	Elongation	Color	Dispersion
Boralsilite	+82°	1.629	0.025	{100}	γ‖*b*	None	*r* > *v*, weak
Sillimanite	+31° to +11°	1.653 to 1.661	0.018 to 0.022	None	γ‖*c*	Rare	*r* > *v*, weak to strong
Werdingite	−33°	1.614	0.037	‖*c*	γ‖*c*	β, yellow	*r* > *v*, strong

Note: Sources of data: Sillimanite from Deer et al. (1982), Evers and Wevers (1984); werdingite from Moore et al. (1990).

them. The Al_2SiO_5 phases are found sparingly in the boralsilite-bearing thin sections, but only in HE138B3 do they occur less than 1 mm from boralsilite. In this section, one or two small Al_2SiO_5 grains are found with dumortierite in the vicinity of boralsilite. The closer grain (0.6 mm from boralsilite, Als, Fig. 2), resembles andalusite optically, whereas the further grain (1 mm from boralsilite) is more like sillimanite. However, the further grain is not exposed on the thin section surface and its composition could not be determined.

PHYSICAL AND OPTICAL PROPERTIES

Boralsilite has a fair prismatic cleavage. The luster is vitreous. Hardness could not be accurately determined because of the small crystal size and common alteration. The streak is presumed to be white because the mineral is colorless. The calculated density is 3.07 g/cm³ (for an average composition of the Larsemann Hills material, $Fe_{0.08}Al_{15.97}B_{6.08}Be_{0.002}Si_{1.92}O_{37}$)

Boralsilite is transparent and colorless in thin section; it is biaxial positive. Optical constants measured at λ = 589 nm on Larsemann Hills material using the spindle stage (Bloss 1981) and dispersion staining technique (Su 1993) are α = 1.629(1), β = 1.640(1), γ = 1.654(1), and $2V_{meas}$ = 81.8(6)°; in addition, *r* > *v* is extremely weak and γ‖*b* (positive elongation). Prisms in the Larsemann Hills sample are commonly twinned. Although boralsilite, werdingite, and sillimanite appear similar in thin section, distinctive characteristics allow identification during a routine petrographic study (Table 2). Calculation of the Gladstone-Dale relationship yields a compatibility index of −0.001, which is in the "superior" category (Mandarino 1981).

Examination of cleavage fragments from both localities spread on holey-C films using a Philips CM-12 transmitting electron microscope (TEM) produced no selected area electron diffraction (SAED) patterns and featureless high resolution images. Presumably, the samples were damaged instantaneously by the electron beam (H. Dong, personal communication).

TABLE 3. Boralsilite powder diffraction data

I	d_{obs}	d_{calc}	*hkl*	*I*	d_{obs}	d_{calc}	*hkl*
5	6.54	6.54	201	30	2.473	2.488	51$\bar{2}$
70	5.41	5.36	20$\bar{2}$			2.473	22$\bar{2}$
100	5.19	5.21	110			2.460	600
		5.18	20$\bar{2}$			2.455	22$\bar{2}$
60	4.95	4.95	11$\bar{1}$	5	2.360*	2.364	31$\bar{5}$
		4.91	111			2.354	20$\bar{6}$†
70	4.31*	4.31	11$\bar{2}$			2.344	51$\bar{3}$
		4.26	112	10	2.231	2.252	11$\bar{6}$
20	3.66	3.64	11$\bar{3}$			2.241	02$\bar{4}$
30	3.59*	3.61	40$\bar{1}$			2.240	60$\bar{3}$
		3.60	31$\bar{1}$			2.224	42$\bar{0}$†
		3.60	113	40	2.162	2.156	22$\bar{4}$†
60	3.378	3.403	20$\bar{4}$			2.153	007
		3.359	40$\bar{2}$			2.145	42$\bar{2}$
30	3.275	3.270	402	30	2.121	2.132	224
10	3.060	3.072	114			2.121	42$\bar{2}$
		3.037	11$\bar{4}$			2.110	40$\bar{6}$
5	2.794	2.824	20$\bar{5}$	20	2.050	2.049	42$\bar{3}$
		2.787	020†			2.048	207
30	2.692	2.682	40$\bar{4}$†			2.046	025
		2.670	31$\bar{4}$			2.044	406†
30	2.605	2.623	11$\bar{5}$	20	1.950		
		2.614	02$\bar{2}$	5	1.847		
		2.603	314	10	1.786		
		2.596	115	5	1.689		
		2.592	404	10	1.641		
		2.583	51$\bar{1}$	30	1.568		
				10	1.542		
				30	1.510		
				20	1.472		
				5	1.446		
				5	1.395		
				30	1.303		

Note: 114.592 mm diameter Gandolfi camera. Intensities visually estimated. Cell parameters: *a* = 14.767, *b* = 5.574, *c* = 15.079 Å, and β = 91.96°. Reflection with *d* = 7.18 Å from kaolinite not included.

* Reflection may have a component from kaolinite.

† Indices suggested on the basis of single-crystal intensity data.

X-RAY CRYSTALLOGRAPHY

Precession and Weissenberg diffraction patterns of crystals from both localities showed that boralsilite is monoclinic, space group *C*2, *Cm*, or *C*2/*m*. Single crystals studied by X-ray diffraction from both localities show the near-universal presence of fine twinning on {100}, which is not always evident optically. Intensities indicated that the relative proportions of the twin domains vary and that twin domains are on the order of tens of micrometers. One crystal from the Larsemann Hills specimen was found to be untwinned and was therefore used for collecting intensity data with an Enraf-Nonius CAD4 4-circle diffractometer. Least-squares refinement of lattice parameters yielded the values *a* = 14.767(1), *b* = 5.574(1), *c* = 15.079 (1) Å, β = 91.96(1)°, *V* = 1240.4 (2) Å³, and *Z* = 2. Determination and refinement of the structure (*R* = 2.6%) confirmed that *C*2/*m* is the correct space group, insofar as this property can be determined by X-ray diffraction (D. Peacor et al., in preparation). Powder diffraction data obtained using a Gandolfi camera are listed in Table 3.

CHEMICAL COMPOSITION

Experimental methods

Constituents with atomic number ≥9 were analyzed with an ARL SEMQ electron microprobe at the Univer-

TABLE 4. SIMS data for boralsilite in specimen 8812905-2 (Larsemann Hills)

	Standard	Grain 1		Grain 3	
		Range	Average	Range	Average
BeO, ppm	Sur	34–53	42 ± 8	34–48	40 ± 7
B_2O_3, wt%	Mix	19.20–21.17	20.07 ± 0.9	18.62–21.55	19.63 ± 1.4
B_2O_3, wt%	Gdd	18.59–21.10	19.64 ± 1.1	18.22–20.52	19.07 ± 1.0

Note: n = number of analyses, Sur = surinamite, Gdd = grandidierite, and Mix = average of tourmaline, prismatine, and grandidierite. Standard deviation is 1 σ_n. Grain 1: $n = 4$ for Be, $n = 5$ for B. Grain 3: $n = 3$ for Be, $n = 4$ for B.

sity of Maine (15 kV accelerating voltage, 10 nA beam current, and 3 μm spot size) and with a JEOL 8900 electron microprobe at the U.S. Geological Survey (10 kV, 30 nA beam current, and 1–2 μm spot size). Both electron microprobes are wavelength dispersive (details are given in Grew et al. 1998). In addition, B was measured with the JEOL microprobe using a Mo/B_4C synthetic multilayer crystal with $2d = 148$ Å and uvite as a B standard (no. NMNH C5212, McGee and Anovitz 1996, Table 2). The NIST glass standard K326, which contains 30.0 wt% B_2O_3 (McGee and Anovitz 1996), was tried as a B standard, but gave less satisfactory results than uvite. Boron peaks were measured using both peak height and peak integration. Electron microprobe analysis (EMPA) of boron is complicated by several other difficulties (McGee and Anovitz 1996). Internal fluorescence of the Mo/B_4C analyzing crystal (Kobayashi et al. 1995; McGee and Anovitz 1996) can contribute a small spurious B signal. The level of this signal varies depending on analytical conditions and the material analyzed. For the analyses reported here, this internal fluorescence may contribute ~0.3% B_2O_3, an estimate based on analyses of B-free standards. However, because the amount of this spurious signal varies (probably due to variations in absorption of the spurious signal by the sample), it is unclear to what extent internal fluorescence contributes to the B signal from B-bearing materials. Other complications may include different background behavior between standards and unknown, especially if they differ in structure (G. Morgan, written communication, 1997). We took these contributions into account in estimating analytical error from measurements of B standards to be ~4–5% relative of EPMA B_2O_3 contents.

Li, Be, and B were analyzed using a Cameca ims 4f ion microprobe (secondary ion mass spectrometry or SIMS) operated on the University of New Mexico (UNM) campus by a UNM-Sandia National Laboratories consortium. The analyses were made under the following operating conditions: $^{16}O^-$ primary beam, nominal 12.5 kV primary acceleration voltage, beam current of 10–20 nA, 20–35 μm spot size, secondary beam voltage offset of 50 V, and an energy window of 25 V. The ion signals of ^7Li, ^9Be, and ^{11}B were normalized to the ^{30}Si signal and SiO_2 content in wt%, and Li, Be, and B contents were calculated from working curves scaled to the factors ($^7Li/^{30}Si)\cdot SiO_2$, ($^9Be/^{30}Si)\cdot SiO_2$, and ($^{11}B/^{30}Si)\cdot SiO_2$ of the standards (Grew et al. 1998). To minimize secondary ion yield matrix effects, it is desirable to match the standards and unknowns in terms of crystal structure and composition, e.g., lithian schorl with 496 ppm Li (John Husler, personnel communication) was used as an Li standard for tourmaline. Lithian schorl and prismatine were averaged for boralsilite, resulting in Li_2O contents 0.0008 wt% or less, i.e., <0.002 wt% Li_2O allowing for uncertainties in standardization with unrelated minerals. Surinamite $(Mg,Fe)_3Al_4BeSi_3O_{16}$ was used as a Be standard; no closer match was available. Because of the possible interference between $^9Be^+$ and $^{27}Al^{3+}$ in the Al-rich mineral boralsilite, Be was also analyzed at a mass resolution $M/\Delta M \approx 1100$, yielding BeO = 0.0037–0.0053 wt% in no. 8812905, values similar to those obtained at $M/\Delta M \approx 320$, the routine experimental conditions (Grew et al. 1998). In the present study, the following revised values were used for three of the four boron standards: 3.06 wt% B in lithian schorl (no. 112566, M. D. Dyar, personal communication); 1.21 and 1.31 wt% B in prismatine (respectively, no. BM1940, 39 and no. 112233, Cooper 1997; cf. Grew et al. 1998). Analyses of B of tourmaline, grandidierite, and two prismatine standards suggested that the matrix effect in these minerals is less significant than other sources of error. This conclusion was also reached by other investigators (Hervig 1996). Measured $(B/Si)\cdot SiO_2$ factors in the standards differed by as much as 12% during any given session, and consequently, it seemed preferable to use working curves based on the average of all four standards. Reproducibility of the SIMS data, which was estimated from repeated analyses of single grains of boralsilite in sample 8812905-2, is ±20% (1σ) of the value for a trace constituent (BeO) and ±4–7% (1σ) of the value for a major constituent (B_2O_3) (Table 4).

Neither EMPA nor SIMS gave satisfactory results for the B_2O_3 content of boralsilite. The problem probably results from using inappropriate standards. Given its high Al and B contents and low Si content, boralsilite differs markedly from the crystalline B standards used in the electron and ion microprobe analyses. The K326 glass differs even more markedly in composition as well as in structure from boralsilite, and thus gave poorer results than uvite with the electron microprobe. The coordination of boron could affect EMPA of boron (McGee and Anovitz 1996). Both $^{[4]}B$ and $^{[3]}B$ are present in boralsilite (Peacor et al., in preparation), whereas only $^{[3]}B$ is present in uvite. In order to minimize the effect of coordination, B was measured by integration of the B $K\alpha$ peak area

TABLE 5. Analyses of boralsilite

	Larsemann Hills					Almgjotheii				Ideal
Section	8812905-1		8812905-2			HE138B3		HE138B2	HE138B1	—
Grain no.	1	1	1	2	3	1	2	1 to 4	1 to 8	—
					EPMA and SIMS (for BeO), wt%					
n	7	9	9	10	10	4	2	4*	15*	—
Probe	ARL	JEOL	ARL	ARL	ARL	JEOL	JEOL	JEOL	JEOL	—
SiO_2	9.32	9.65	9.56	10.76	10.05	12.67	10.77	10.68	10.52	10.498
P_2O_5	—	≤0.02	—	—	—	bld.	bld.	bld.	bld.	—
Al_2O_3	70.54	69.47	71.42	71.50	71.23	69.15	70.58	70.00	69.91	71.257
FeO	0.26	0.47	0.51	0.46	0.48	1.10	0.83	1.04	0.89	—
MgO	bld.	0.01	bld.	bld.	bld.	0.23	0.11	0.17	0.18	—
BeO	0.003‡	0.003‡	0.004	0.004	0.004	0.094	0.084	0.25	—	—
					B_2O_3, wt%					
EPMA	—	16.99	—	—	—	14.83	15.92	16.03	17.77†	—
SIMS	18.00‡	18.64‡	20.07	20.83	19.63	18.11	19.38	19.71	—	—
Calc§	18.625	18.150	18.835	18.270	18.530	16.775	18.085	18.065	17.980	18.245
Total§	98.75	97.75	100.33	100.99	100.29	100.02	100.46	100.21	99.48	100.0
					Formulae per 37 O atoms					
Si	1.798	1.884	1.818	2.035	1.913	2.435	2.052	2.041	2.025	2.0
Be	0.001	0.001	0.002	0.002	0.002	0.043	0.038	0.115	—	0
B(calc)§	6.202	6.116	6.182	5.965	6.087	5.565	5.948	5.959	5.975	6.0
Al	16.038	15.984	16.006	15.939	15.977	15.664	15.849	15.766	15.862	16.0
Fe	0.042	0.077	0.081	0.073	0.076	0.177	0.132	0.166	0.143	0
Mg	0	0.003	0	0	0	0.066	0.031	0.048	0.052	0
Total	24.081	24.065	24.089	24.014	24.055	23.950	24.050	24.095	24.057	24.0

Note: EMPA = electron microprobe analysis, SIMS = secondary ion mass spectroscopy (ion probe), bld. = below limits of detection, dash = no data, *n* = number of analyses averaged. MnO, CaO, Na_2O, K_2O, F, Cl, P_2O_5, TiO_2 are at limit of detection. Li_2O detected by SIMS, but is <0.002 wt%. Fe assumed to be ferrous.

* Only analyses with SiO_2 <11% used in average (all analyses are plotted in Fig. 5).

† B_2O_3 from peak height instead of peak integration.

‡ One SIMS analysis applied to two different EMPA.

§ Boron calculated from B + Si = 8 apfu. Analytical totals based on the calculated B_2O_3.

rather than by its height during a second session on the JEOL instrument (Table 5, Fig. 5A). The resulting B contents and analytical totals are systematically low, whereas peak height data gave "reasonable" B contents and totals, i.e., B + Si ≈ 8 apfu (see below). The SIMS B contents are systematically high relative to the ideal formulation and result in high analytical totals (101.35 to 103.55 wt% excluding sample no. 8812905-1). Inasmuch as grandidierite is closer to boralsilite structurally and chemically than either tourmaline or prismatine, SIMS B_2O_3 contents were also calculated using only grandidierite as a standard, but this results in little improvement (Table 4). Apparently, the ion yield of B relative to Si is higher in boralsilite than in the ferromagnesian borosilicates used as standards including grandidierite, that is, a matrix effect comes into play when differences in composition are substantial. Given these analytical difficulties, B_2O_3 contents of boralsilite were calculated assuming B + Si = 8 (Table 5).

Boralsilite

The major constituents of boralsilite from Larsemann Hills are SiO_2, Al_2O_3, and B_2O_3; FeO is a minor, and BeO is a trace constituent (Table 5). The low analytical totals reported for one section (columns 1–2) could be due to submicroscopic secondary hydrous phases. The SiO_2 and Al_2O_3 contents of three grains in the second section (columns 3–5) approach closely the values calculated from $Al_{16}B_6Si_2O_{37}$, which is the formula obtained from crystal structure refinement of the Larsemann Hills specimen (D. Peacor et al., in preparation).

The Almgjotheii boralsilite (HE138B) differs in containing more SiO_2, BeO, and FeO; less Al_2O_3 and B_2O_3; and measurable MgO; it is noticeably heterogeneous. Compositions obtained from EPMA (Fig. 5) show a greater range than expected from analytical error or difficulties with B analysis, e.g., SiO_2 9.66–13.17 wt% and B_2O_3 14.59–18.45 wt%. Inasmuch as the JEOL data were obtained under the same analytical conditions of B during a given session (either peak height or peak integration), the trends of each session are presumed to reflect real variations. The clearest trend among major constituents is the inverse relation between B and Si, roughly SiB_{-1} (Fig. 5A), and for this reason, the B_2O_3 contents of boralsilite listed in Table 5 were calculated assuming Si + B = 8 apfu. This trend appears to result largely from solid solution of boralsilite with sillimanite or $Al_8B_2Si_2O_{19}$, a "boron-mullite" synthesized by Werding and Schreyer (1992). No trend is evident between Mg + Fe and Si (Fig. 5B). If werdingite impurities or solid solution played the dominant role, the points would follow a trend parallel to $(Mg,Fe)SiAl_{-1}B_{-1}$. Figure 5C suggests an indistinct inverse relationship between Al and Si that is intermediate between the exchanges $SiAl_{-0.22}$ for boralsilite-Al_2SiO_5 (or $Al_8B_2Si_2O_{19}$) solid solution and $SiAl_{-1}$ for boralsilite-werdingite solid solution (cf. $SiAl_{-2}$ for the Tschermaks sub-

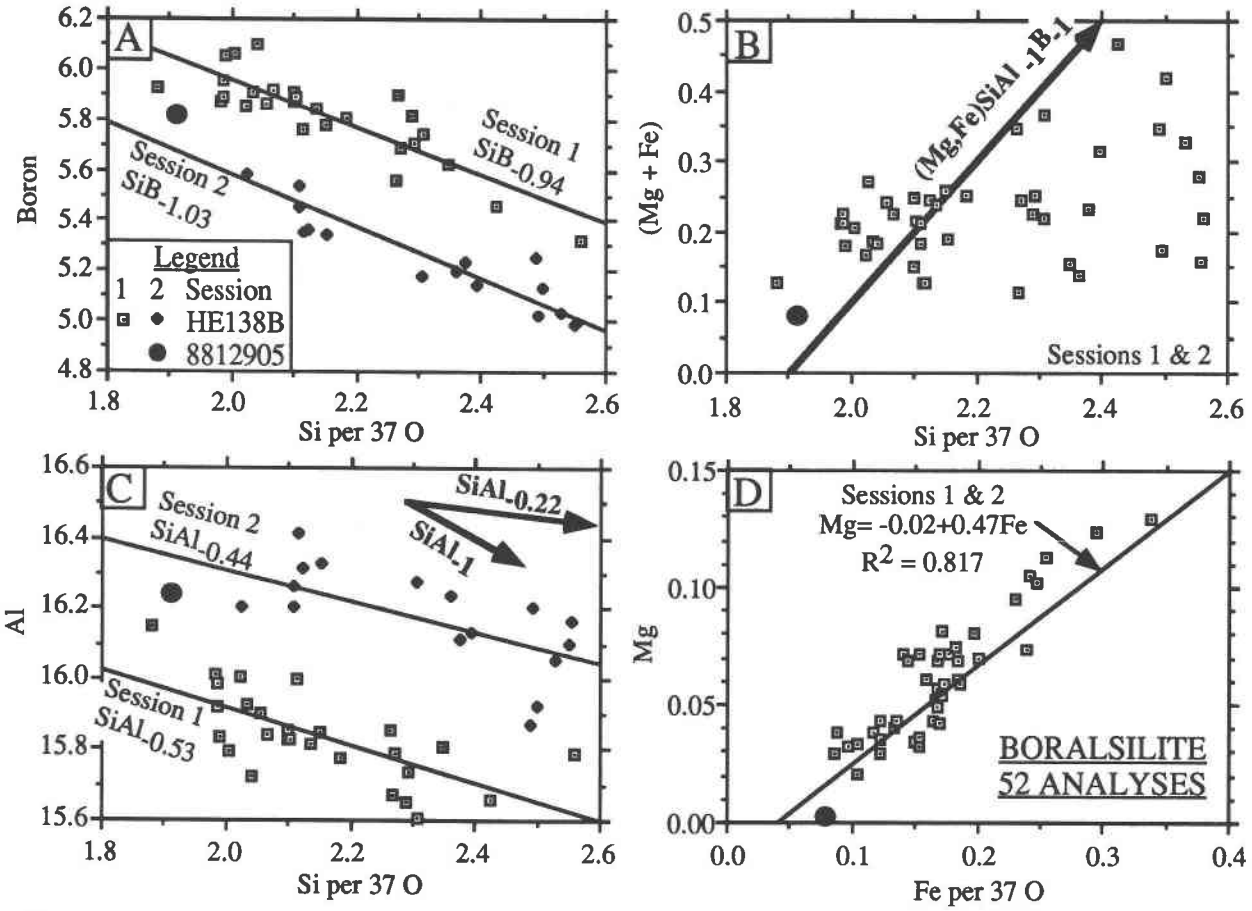

FIGURE 5. Electron microprobe data for boralsilite in no. HE138B (43 individual analyses including those averaged in Table 5) and no. 8812905 (average of 9 analyses, Table 5) obtained with the JEOL instrument (MnO, TiO_2, and BeO contents ignored). Session 1: Boron content determined from peak height (open symbols in A and C). Session 2: Boron content determined from integrated peak area (filled symbols in A and C). Lines in A, C, and D are least-squares fits. Idealized substitutions are shown as bold arrows.

stitution). Mg increases regularly with Fe with X_{Fe} = Fe/(Mg + Fe) ≈0.68 (Fig. 5d), which is bracketed by the average X_{Fe} = 0.60–0.74 in associated werdingite (Grew et al. 1998).

TABLE 6. EPMA of dumortierite in HE138B3

	Weight percentage			Formulae for 17.625 O atoms	
	Blue	Rose		Blue	Rose
n	5	6	Si	2.954	2.934
SiO_2	31.29	30.94	B	1.030	1.023
TiO_2	0.23	4.02	Al	6.704	6.389
B_2O_3	6.32	6.25	Ti	0.016	0.287
Al_2O_3	60.26	57.16	Fe	0.034	0.021
FeO	0.43	0.26	Mg	0.049	0.045
MgO	0.35	0.32	Total	10.787	10.699
H_2O*	1.19	1.19	OH	0.75	0.75
Total	100.07	100.14			

Note: JEOL instrument was used. *n* = number of analyses. P_2O_5, MnO, CaO, Na_2O, K_2O, F are at detection limit. Fe assumed to be ferrous.
* H_2O is calculated assuming O = 17.250 and OH = 0.75.

Grandidierite, sillimanite, andalusite, dumortierite, and tourmaline

In the samples from Almgjotheii, grandidierite is ferroan (Fe/(Fe+Mg) = 0.50–0.67), and the Al_2SiO_5 phases are relatively poor in Fe_2O_3, 0.33–0.34 wt% (Grew et al. 1998). These authors also reported 0.46 wt% B_2O_3 in sillimanite, but only 0.004 wt% B_2O_3 in andalusite. The blue dumortierite that is closely associated with boralsilite at Almgjotheii (e.g., Fig. 2) is depleted in Ti and enriched in Al compared to the pink variety (Table 6).

Tourmaline is compositionally heterogeneous (Table 7; Fig. 6). At one extreme is the early formed, moderate- to dark-olive tourmaline in the Larsemann Hills sample; at the other extreme is the blue tourmaline adjacent to boralsilite, which is characterized by high-Al content, depletion in Mg and Ti, and by 50% vacancies on the alkali (*X*) site (Fig. 6A). The early formed tourmaline is largely schorl-dravite; the blue tourmaline approaches the foitite-olenite join (Fig. 6B). Li contents are too low (0–0.028 Li apfu) for involvement of the elbaite substitution Li-

TABLE 7. Representative analyses of tourmaline

	Larsemann Hills, Specimen 8812905						Almgjotheii	
Section no.	1	2	2	1	1	1	HE138B2	HE138B2
Grain	1-core	1-margin	1-core	4	3	2a		
Color	olive	pale/Bor*	blue	blue	olive	olive	blue/Bor*	blue/Gdd†
				EMPA (ARL probe) wt%				
n	10	10	10	10	10	10	7	6
SiO_2	34.39	34.92	34.19	36.11	33.59	34.51	35.25	35.69
TiO_2	0.68	bld.	bld.	0.17	1.49	1.65	bld.	0.14
Al_2O_3	36.71	37.12	32.59	34.76	31.63	30.50	37.84	34.16
FeO	9.75	12.17	17.30	11.41	13.98	9.03	10.27	10.81
MnO	bld.	bld.	bld.	bld.	bld.	bld.	bld.	bld.
MgO	2.16	bld.	bld.	2.19	2.35	6.66	0.67	3.28
CaO	0.45	0.21	0.79	0.04	1.16	1.51	bld.	0.08
Na_2O	1.78	1.31	1.46	1.22	1.92	1.87	1.36	1.47
K_2O	0.05	bld.	0.03	0.01	0.10	0.10	0.02	0.02
F	—	—	—	bld.	bld.	0.21	bld.	bld.
				SIMS, wt%				
Li_2O	0.022	0.042	0.010	0.001	0.007	0.003	0.004‡	0.0003‡
BeO	0.0002	0.001	0.002	0.0001	0.0001	0.0001	0.001‡	0.0002‡
B_2O_3	11.40	11.07	10.53	10.52	10.40	10.83	10.06‡	10.31‡
				Calculated wt%				
H_2O	3.68	3.64	3.52	3.62	3.53	3.51	3.61	3.60
O = F	—	—	—	0	0	−0.09	0	0
Total	101.07	100.48	100.42	100.05	100.16	100.29	99.08	99.56
				Formulae for 29 O				
Si	5.607	5.758	5.831	5.977	5.708	5.737	5.862	5.944
Be	0	0	0.001	0	0	0	0	0
B	3.208	3.151	3.100	3.006	3.051	3.108	2.888	2.964
Al	7.054	7.213	6.551	6.781	6.335	5.976	7.417	6.705
Ti	0.083	0	0	0.021	0.190	0.206	0	0.018
Fe	1.329	1.678	2.468	1.579	1.987	1.255	1.428	1.506
Mg	0.525	0	0	0.540	0.595	1.651	0.166	0.814
Li	0.014	0.028	0.007	0.001	0.005	0.002	0.003	0
Ca	0.079	0.037	0.144	0.007	0.211	0.269	0	0.014
Na	0.563	0.419	0.483	0.392	0.633	0.603	0.439	0.475
K	0.010	0	0.007	0.002	0.022	0.021	0.004	0.004
Total	18.472	18.284	18.592	18.306	18.737	18.828	18.207	18.444
F	—	—	—	0	0	0.110	0	0
OH	4	4	4	4	4	3.890	4	4
X_{Mg}	0.28	0	0	0.25	0.23	0.57	0.10	0.35

Note: EMPA = electron microprobe analysis, SIMS = secondary ion mass spectroscopy (ion probe), bld, below limits of detection, dash = no data. *n* = number of analyses. Fe assumed to be ferrous.

* Adjacent to boralsilite (e.g., Fig. 2).

† Adjacent to grandidierite.

‡ One SIMS analysis had been applied to 2–3 different zones in one grain.

$AlFe_{-2}$ in Al enrichment. The low-Fe_2O_3 contents in associated Al_2SiO_5 phases in the Almgjotheii sample suggest that Fe^{3+} plays a minor role in the Almgjotheii tourmaline. There is no evidence for unusually oxidizing conditions in the Larsemann Hills sample, and significant Fe^{3+} substitution seems unlikely in this sample as well. Although some $^{[4]}Al$ appears to substitute for Si, the dominant substitutions introducing Al into tourmaline are most likely $[\square Al][Na(Fe^{2+},Mg)]_{-1}$ and $(AlO)[(Fe^{2+},Mg)\text{-}OH]_{-1}$, which involve Al on octahedral sites (Fig. 6B; Burt 1989; London and Manning 1995). The latter substitution is a deprotonation, implying that the highly aluminous tourmaline has less than 4(OH,F) apfu.

PARAGENESES

Geologic situation and conditions of formation

The boralsilite-bearing pegmatites at both localities are interpreted to be partial melts intruded during heating after the peak metamorphic event (Stüwe et al. 1989; Dirks et al. 1993; Carson et al. 1997; Huijsmans et al. 1981, 1982, see also Grew et al. 1998). Host rocks are polymetamorphic granulite-facies rocks of late Proterozoic age. However, the localities differ in other respects.

Larsemann Hills, Antarctica. The Stornes Peninsula is remarkable for borosilicate enrichment in localized domains in the host gneisses (Ren et al. 1992; Ren and Liu 1994; Carson et al. 1995). Tourmaline, prismatine, (a B-rich analogue of kornerupine, Grew et al. 1996), and grandidierite are widespread; the last two are inferred to have crystallized coevally at about 750 °C and 4–5.5 kbar (Ren et al. 1992; Carson et al. 1995). The boralsilite-bearing tourmaline-quartz intergrowth occurs as a patch in a layer-parallel, locally discordant pegmatitic mass in cordierite ± garnet-sillimanite gneisses. This pegmatitic mass is probably related to the partial melts that formed during decompression from peak conditions (D2) at about 7 kbar and about 800 °C to 4–5 kbar at about 750 °C and low P_{H_2O} (D2–D3, Carson et al. 1997; cf. Stüwe and Powell 1989a, 1989b; Stüwe et al. 1989). The source of boron for the boralsilite-bearing pegmatite was most likely the

precursor to the boron-rich domains in the host gneisses. Boron enrichment in these domains could have been a primary (sedimentary) feature in rocks on the Stornes Peninsula (Carson et al. 1995).

Textures in the boralsilite-bearing specimen suggest that the first generation schorl-dravite, quartz, and potassium feldspar are early formed magmatic minerals. Boralsilite is probably early and magmatic as well. Assuming that the pegmatite formed near the end of decompression, we conclude that boralsilite crystallized at about 750 °C and 4–5 kbar. The olenite-foitite tourmaline probably formed in localized chemical environments developed around boralsilite and potassium feldspar during later retrogression of the pegmatite. London and Manning (1995) reported Al-rich, alkali-deficient tourmalines in granites and associated rocks from southwestern England and concluded that increasing tourmaline Al content is associated with increasing Al and B activity in the melt from which the tourmaline crystallized. B_2O_3 and Al_2O_3 activities in the immediate vicinity of boralsilite should have been exceptionally high, and this is reflected in tourmaline compositions even more Al-rich and alkali-deficient than those reported by London and Manning (1995). Alkali deficiency in tourmaline is not necessarily a result of low temperatures (Werding and Schreyer 1984; Sperlich et al. 1996), although such tourmalines are commonly found in low-temperature environments (e.g., Henry and Dutrow 1996; Novoselova and Sosedko 1991)

Almgjotheii, Rogaland, Norway. The Almgjotheii pegmatite was emplaced during the third metamorphic event to affect the Rogaland aureole (M3), which is correlated with deformation (D3) during final stages of emplacement of the anorthosite (Maijer et al. 1981; Maijer 1987; Huijsmans et al. 1981, 1982; Grew et al. 1998). Conditions during M3 are inferred to have been T = 550–700 °C and P = 3–5 kbar (Jansen et al. 1985; Wilmart and Duchesne 1987). Grew et al. (1998) proposed the following sequence of crystallization based on textural evidence: (1) rose-colored Ti-rich dumortierite (Dum I), andalusite I, sillimanite (?), grandidierite, and garnet; (2) werdingite, boralsilite, blue-purple Ti-poor dumortierite (Dum II), sillimanite, grandidierite II (?) grading into (3) tourmaline, corundum, hercynite, sillimanite, andalusite II, more dumortierite II; and (4) hydrous phyllosilicates, including sericite, chlorite, and margarite. Textures suggest that the minerals of group 1 are magmatic, whereas those in the other three groups most likely formed by reactions among the early formed magmatic minerals or between these minerals and fluids. The occurrence of boralsilite as overgrowths on grandidierite suggests that it could have formed by reaction of grandidierite with a B-rich residual fluid or with Ti-rich dumortierite (Dum I). As sillimanite also occurs as overgrowths on grandidierite, boralsilite is most likely coeval with sillimanite. Tourmaline overgrows boralsilite-werdingite intergrowths, implying tourmaline formed later than boralsilite, whereas low-Ti dumortierite appears to be largely coeval with boralsilite. As in the case at Larsemann Hills, B_2O_3 and Al_2O_3 activities in the immediate vicinity of boralsilite resulted in Al-rich tourmaline; the Al-rich environment is also reflected in Al-rich, Ti-poor dumortierite.

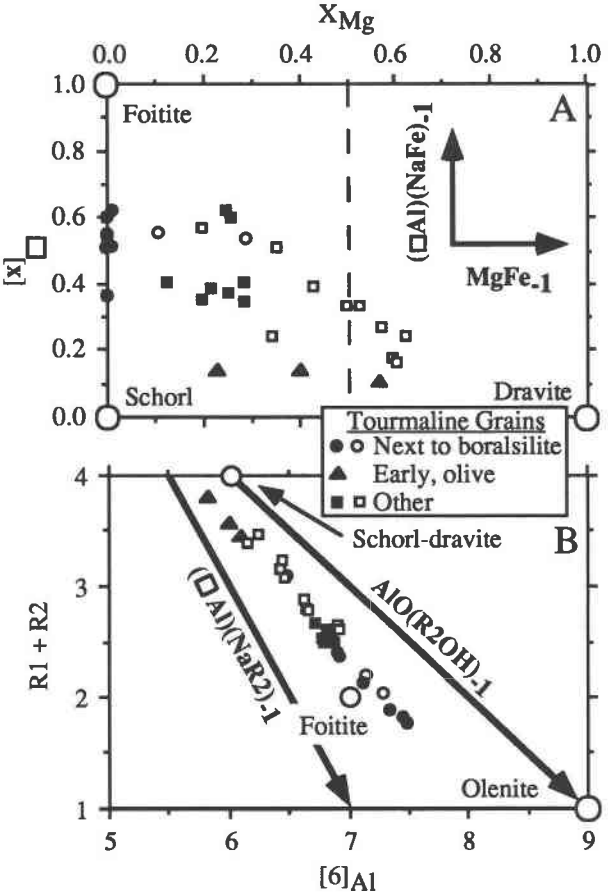

FIGURE 6. Compositional data for tourmaline (30 EPMA and 10 SIMS analyses) from Table 7, Grew, Yates, Shearer, and Wiedenbeck (unpublished data), Huijsmans (1981) and Huijsmans et al. (1982). Filled symbols = Larsemann Hills; open symbols = Almgjotheii; large circles = tourmaline end-members. Idealized substitutions are shown bold. (**A**) follows Henry and Dutrow (1996, Fig. 11). (**B**) follows London and Manning (1995, Fig. 3A), except Ti is not included. R1 = Na + Ca + K apfu. R2 = Mg + Fe (+Mn) apfu. $^{[6]}$Al = Si + Al + B − 9 apfu, where measured B content is used except when measured B < 3 apfu, then B = 3 apfu as was assumed for tourmaline in which B was not measured.

Boralsilite is inferred to have formed at $T \approx$ 600–700 °C and $P \approx$ 3–4 kbar. The presence of andalusite + potassium feldspar restricts total pressure to 3–4 kbar and $X_{H_2O} < 0.5$ in the associated fluid phase (Kerrick 1972), that is, relatively dry conditions. In estimating the pressure, we have taken into account a possible shift of the Al_2SiO_5 triple point because of the presence of boron in sillimanite and its absence in andalusite or kyanite. Using idealized compositions of the Almgjotheii sillimanite and andalusite, respectively, $^{[6]}Al_{0.993}{}^{[4]}AlSi_{0.977}O_{4.855}$ and $^{[6]}Al_{0.993}{}^{[4]}AlSiO_5$ (Grew et al. 1998, Table 6), the relation-

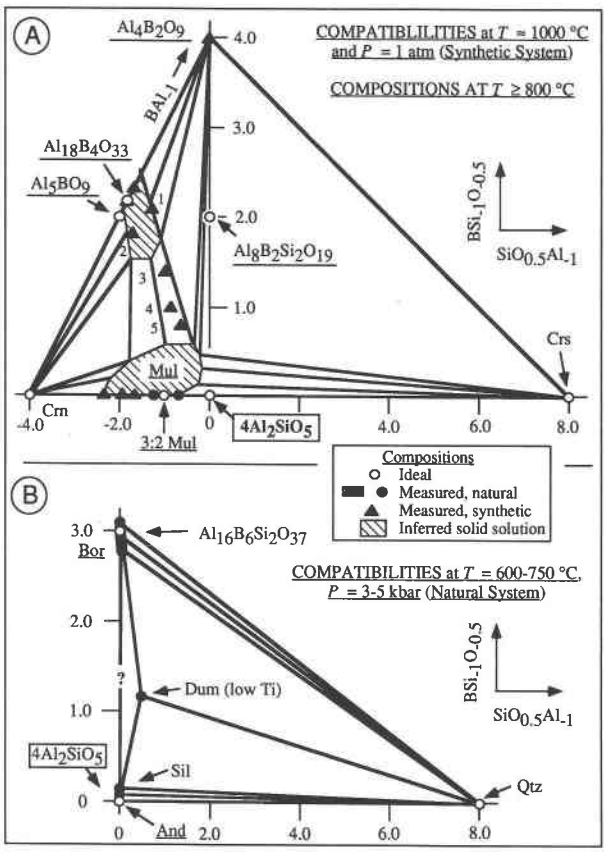

FIGURE 7. "Boron-mullites", aluminum borates and associated phases in the B_2O_3-poor portion of the Al_2O_3-B_2O_3-SiO_2 system. The natural compatibilities (**B**) and compositions (except mullite) are taken from Figure 8 and Tables 5 and 6. The compatibilities for $T \approx 1000$ °C (**A**) are based on the experiments of Kim (1961), Gielisse (1961), and Gielisse and Foster (1961, 1962). Compositional ranges are conjectural. Mul = mullite; Crs = cristobalite. Other mineral abbreviations are given in Table 1. Underlining indicates phases with structures related to sillimanite. The aluminoborate-mullite solid solutions were synthesized at the following temperatures: 1 = 930 °C, Letort (1952); 2 = 1200 °C, Gelsdorf et al. (1958); 3 = 1525 °C, 4 = 1555 °C, and 5 = 1605 °C, i.e., samples were annealed about 50 °C below the liquidus, Dietzel and Scholze (1955). Sources of compositional data for aluminoborates, $Al_8B_2Si_2O_{19}$, and mullite are, respectively, Ihara et al. (1980), Scholze (1956), Sokolova et al. (1978), Werding and Schreyer (1992), Cameron (1977), and Deer et al. (1982). Not shown is a metastable mullite-like binary solid solution from Al_5BO_9 to $AlBO_3$ at $T = 850$–900 °C (Mazza et al. 1992).

ship $\Delta V \Delta P = RT\ln(a_{Sil}/a_{And})$, and a simplified ideal activity model of Al_2SiO_5, $a_{Al_2SiO_5} = (X_{[6]Al})(X_{[4]Al})(X_{Si})(X_O)^5$, we calculate that the andalusite-sillimanite boundary shifts −1.6 kbar at 700 °C, and the triple point pressure, about −0.5 kbar (Kerrick 1990, Fig. 4.40), i.e., to 3.4–4 kbar from the 4.2 ± 0.3 kbar Al_2SiO_5 triple point of Bohlen et al. (1991). As muscovite B_2O_3 contents exceed the B_2O_3 contents of quartz, andalusite and most potassium feldspar (Grew 1996), muscovite would be stabilized to higher temperatures in a B-rich system and its breakdown in the andalusite stability field would require lower H_2O activities than that given by Kerrick (1972) for the B-free system.

Phase relationships and related experimental work

Experimental systems relevant to boralsilite include (1) granitic, (2) Al_2O_3-B_2O_3-SiO_2 ± H_2O, and (3) MgO-FeO-Al_2O_3-B_2O_3-SiO_2-H_2O. Evidence that the acicular phases reported in some experimental studies of boron-bearing granitic systems is boralsilite or a related phase is equivocal. Pichavant (1979, 1981) and Dingwell et al. (1996, Fig. 22a) reported an acicular unknown formed by heating a gel of granitic composition containing 0–18 wt% B_2O_3 to $T = 500$–740 °C and $P_{H_2O} = 1$ kbar (vapor saturation); the unknown was best developed in B-rich experiments. Electron microprobe data ($SiO_2 \approx 30$ wt%, $Al_2O_3 \approx 50$ wt%) and a Raman spectrum were cited to suggest that the acicular phase was a ternary Al_2O_3-B_2O_3-SiO_2 solid solution. Dingwell et al. (1996) presumed the acicular phase to be a Na-Al tourmaline similar to the Na-Al tourmaline synthesized by Rosenberg et al. (1986) at 450–600 °C (subsolidus) and $P_{H_2O} = 1$ kbar. The Raman spectrum (Pichavant 1979, Fig. 54a) is not sufficiently diagnostic to conclusively identify the unknown as tourmaline, although it is sufficiently distinctive to justify Pichavant's (1979) conclusion that the unknown is not sillimanite. Moreover, the appearance of this unknown in gels lacking B implies either that B is a non-essential constituent or that there are two unknowns. Chorlton (1973) and Chorlton and Martin (1978) reported a weakly pleochroic blue-green acicular phase formed by the dry melting of a tourmaline-bearing granite (1.74 wt% B_2O_3, 20–25% Tur) at $T = 841$–1100 °C (beginning of melting between 858 and 877 °C) and $P = 1$ atm. The three to five peaks in the X-ray diffraction patterns could be from grandidierite, which is blue-green, or from a phase related to sillimanite, i.e., mullite, werdingite, boralsilite, or a "boron-mullite."

Because of its importance to the glass and ceramics industry, the Al_2O_3-B_2O_3-SiO_2 ± H_2O system has been studied fairly extensively at high temperatures ($T \geq 800$ °C, Fig. 7A). The binary and ternary compounds in this diagram are anhydrous orthorhombic phases; Werding and Schreyer (1984, 1996) termed the ternary phases "boron-mullite" because of their structural affinities with sillimanite and mullite. Only one of these compounds has been synthesized under geologically reasonable conditions: $Al_8Si_2B_2O_{19}$ at 800–830 °C and 1–4 kbar (Werding and Schreyer 1992). None of these compounds have been found in nature, and solid solution is much less extensive in the natural compounds than in the synthetic ones. The maximum B_2O_3 contents reported for sillimanite and natural mullite are 0.66 and 0.6 wt%, respectively, and the analyzed mullite could have had a dumortierite impurity (Grew 1996; Grew et al. 1998; Beyer and Schnorrer-Köhler 1981). The maximum sillimanite B_2O_3 content corresponds to $0.13BSi_{-1}O_{-0.5}$ substitution in $4Al_2SiO_5$ (Fig.

7B). Boralsilite shows solid solution corresponding to a range of 0.35 $SiB_{-1}O_{0.5}$ in Figure 7B, in part due to substitutions involving FeO and MgO (Fig. 5).

Subsequent to the discovery of boralsilite, Werding and Schreyer (personal communication) successfully synthesized a monoclinic phase in the system Al_2O_3-B_2O_3-SiO_2. This phase has the same X-ray diffraction pattern as boralsilite. SIMS data gave B/Si ratios comparable to those in natural boralsilite (E. Grew et al., unpublished data). Werding and Schreyer's (personal communication) starting gels had compositions corresponding to $Al_{16}B_6Si_2O_{37}$ and $Al_8B_2Si_2O_{19}$ (plus excess H_3BO_3 to provide a fluid phase). The hydrothermal synthesis was carried out at 1–4 kbar and 700–800 °C, conditions close to those inferred for natural boralsilite.

At temperatures near 1000 °C and atmospheric pressure, only B-poor mullite and $Al_4B_2O_9$ are stable with SiO_2 (Fig. 7A). At geologically more reasonable temperatures and pressures, dumortierite and boralsilite are stable with quartz (Fig. 7B) and thus are the most likely aluminum borosilicate phases to crystallize with sillimanite (or andalusite) in granitic melts that are depleted in components needed for tourmaline and other ferromagnesian borosilicates.

A more complete representation of natural boralsilite composition and assemblages is the model system FeO-MgO-Na_2O-Al_2O_3-B_2O_3-SiO_2 open to water and with excess quartz and albite (Fig. 8). The minerals are plotted in terms of one additive and two exchange components (Thompson 1982) appropriate for sillimanite and related minerals (Werding and Schreyer 1992, 1996). Ideally, sillimanite and related minerals plot in one plane (for a given Mg/Fe ratio).

Boralsilite is in direct contact with quartz, potassium feldspar, plagioclase, grandidierite, werdingite, and tourmaline, and it occurs only a few hundredths of a millimeter from dumortierite. No sillimanite- or andalusite-boralsilite contacts were found, but these phases are found in close proximity, and the coexistence of boralsilite with sillimanite and andalusite is possible. Garnet is abundant in the Almgjotheii pegmatite, but there is no evidence of the coexistence of boralsilite with garnet; there is also no evidence of coexistence of boralsilite with muscovite or cordierite. The absence of boralsilite in garnet-bearing pegmatite can be explained by the presence of the assemblages Tur + Sil, Gdd + Sil, Tur + Dum, and Gdd + Dum, which act as barriers between B-poor assemblages and B-rich assemblages (Fig. 8). Theoretically, at bulk Fe/Mg ratios higher than those attained in the studied pegmatites, the B-rich minerals could coexist with almandine, which has a higher Fe/Mg ratio than associated grandidierite and tourmaline. However, there is no bulk Fe/Mg ratio at which boralsilite could coexist with cordierite because nearly Fe-free grandidierite and dravite are known (Grew 1996; Henry and Dutrow 1996).

The following assemblages with the fewest degrees of freedom are inferred to have been stable: (1) Qtz + Kfs + Bor + schorl-dravite (8812905); (2) Kfs + Pl(An_{22}) + Bor + Wrd + Dum + Gdd (HE138B1, Fig. 4); (3) Qtz + Kfs + Bor + Dum + Al_2SiO_5 (HE138B3, Fig. 2). Whether quartz is also a part of assemblage 2 is problematic; it surrounds the borosilicate aggregate, but is rare inside it. Elsewhere in HE138B, the borosilicates are in contact with quartz, but at most only three borosilicates are present together.

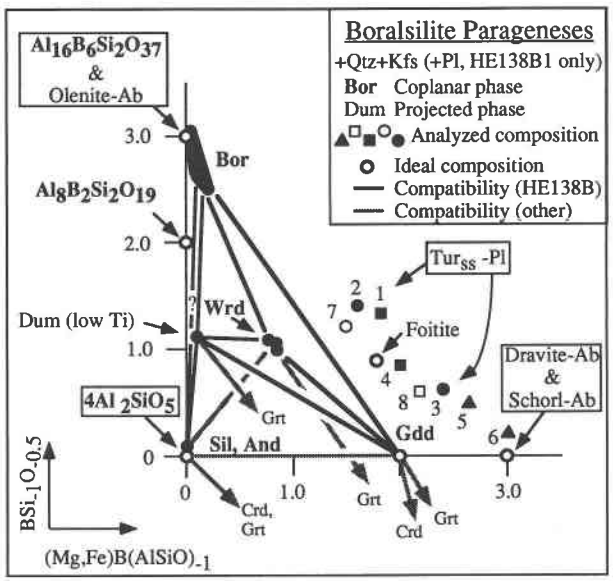

Figure 8. Parageneses in the FeO-MgO-Na_2O-Al_2O_3-B_2O_3-SiO_2-H_2O system. Coplanar phases are minerals with structures related to sillimanite; compositions of the other minerals are projected through quartz onto this plane. Na-Ca tourmalines are also projected through plagioclase (−Ab, −Pl). The mineral abbreviations are given in Table 1; Ab = albite; Crd = cordierite. Sources of compositional data are Figure 5 and Tables 5, 6, and 7 (this paper; numbered tourmaline analyses Tur_{ss} refer to columns in Table 7 and symbols correspond to those in Fig. 6), and Tables 3 and 6 (Grew et al. 1998). Other compatibilities (shown in gray) refer to assemblages found in other specimens.

The observed textures and compositions in assemblage 1 can be interpreted as olenite-foitite tourmaline replacing a primary boralsilite + schorl-dravite + potassium feldspar assemblage of which a simplified reaction can be written:

$$\underset{\text{Bor}}{Al_{16}B_6Si_2O_{37}} + 2\underset{\text{Schorl}}{NaFe_3Al_6(BO_3)_3[Si_6O_{18}](OH)_4} + 4\underset{\text{Qtz}}{SiO_2} + 2\underset{\text{Kfs}}{KAlSi_3O_8} + 2\underset{\text{water}}{H_2O} = 4\underset{\text{Olenite-Foitite}}{Na_{0.5}Fe_{1.5}Al_{7.5}(BO_3)_3[Si_6O_{18}]O(OH)_3} + \underset{K^+ \text{ in solution}}{K_2O} \quad (1)$$

This reaction is evident as the collinear disposition of boralsilite, schorl, and olenite-foitite in Figure 8. The assemblage Bor + Pl + Qtz (cf. assemblage 2) is compositionally equivalent to olenite:

$$\underset{\text{Olenite}}{2NaAl_3Al_6(BO_3)_3[Si_6O_{18}]O_3(OH)} = \underset{\text{Bor}}{Al_{16}B_6Si_2O_{37}} + \underset{\text{Ab}}{2NaAlSi_3O_8} + \underset{\text{Qtz}}{4SiO_2} + \underset{\text{water}}{H_2O} \quad (2)$$

implying that boralsilite would require even lower water activites than the highly deprotonated tourmaline olenite. Assemblage 3 suggests that dumortierite breaks down at temperatures near 600 °C (or less for andalusite to appear) as follows:

$$\underset{\text{Dum}}{6Al_{6.7}BSi_3O_{17.25}(OH)_{0.75}} = \underset{\text{Sil, And}}{12.1Al_2SiO_5} + \underset{\text{Bor}}{Al_{16}B_6Si_2O_{37}} + \underset{\text{Qtz}}{3.9SiO_2} + \underset{\text{water}}{2.25H_2O} \quad (3)$$

Werding and Schreyer (1996) reported that dumortierite breaks down to a "boron-mullite," quartz, and fluid in hydrothermal experiments at 720–830 °C and 2–7 kbar. Because no B-poor aluminosilicate phase formed with quartz, Werding and Schreyer (1996) inferred that this "boron-mullite" was poorer in boron than $Al_8B_2Si_2O_{19}$. Reactions 1–3 have one important feature in common: the Al-B-rich phases alternative to boralsilite, i.e., olenite and dumortierite are hydrous, and formation of boralsilite invariably involves dehydration. This relationship is consistent with boralsilite being favored by $P_{H_2O} < P_{tot}$.

Boralsilite would be expected to crystallize from magmas extremely enriched in Al and B. London and Manning (1995) explained increasing Al content (olenite component) in Li-poor tourmaline to increasing B content of magma in a suite of granitic rocks in southwestern England, i.e., Al-enriched phases are associated with B-rich magma. Al and B contents of a pegmatitic magma could also be enhanced by early crystallization of a ferromagnesian phase such as tourmaline, grandidierite, or garnet. London and Manning (1995) suggested that precipitation of tourmaline from a peraluminous granitic magma could leave the magma depleted in MgO and FeO, but not in B_2O_3; this depletion must be extreme to suppress the formation of schorl-dravite tourmaline in B-Al-rich melts (Wolf and London 1997). An example of this effect is variation in tourmaline composition in the Bob Ingersoll pegmatite, South Dakota. Early Fe-Mg-rich tourmaline is followed by increasingly Li-Al-rich and (Fe,Mg)-poor tourmalines approaching the elbaite end-member (Jolliff et al. 1986). If Li is absent, the temperatures sufficiently high, and if $P_{H_2O} < P_{tot}$, grandidierite, dumortierite, werdingite, or boralsilite might crystallize instead of aluminous tourmaline. In the case of the Larsemann Hills pegmatite, early crystallization of schorl-dravite could have sufficiently depleted the magma in MgO and FeO for boralsilite to form from B and Al in the residual melt. The highly localized appearance of boralsilite at Almgjotheii can be interpreted by an analogous scenario. In this case, the early formed ferromagnesian phases are grandidierite and garnet. B_2O_3-enriched, MgO-FeO-depleted residual fluids reacted with grandidierite in garnet-free portions of the pegmatite to form boralsilite and werdingite.

Acknowledgments

We thank Mark Cooper, Darby Dyar, and John Husler for unpublished Li and B data on the minerals used as SIMS standards, Hailiang Dong for TEM work on boralsilite, Werner Schreyer and Günter Werding for permission to cite unpublished experimental data on synthetic boralsilite. The thoughtful and detailed comments on earlier drafts by Barbara Dutrow, Charles Guidotti, George Morgan, and Werner Schreyer are gratefully acknowledged. This research was supported by NSF grants EAR-9118408 and EAR-9526403 to the University of Maine. University of New Mexico/Sandia National Laboratories SIMS facility is a national user facility supported in part by NSF grant EAR-9506611.

References cited

Beyer, H. and Schnorrer-Köhler, G. (1981) Jeremejewit-Neufund in der Eifel. Aufschluss, 32, 125–129.

Bloss, F.D. (1981) The spindle stage: Principles and practice, 340 p. Cambridge University Press, Cambridge.

Bohlen, S.R., Montana, A., and Kerrick, D.M. (1991) Precise determinations of the equilibria kyanite ↔ sillimanite and kyanite ↔ andalusite and a revised triple point for Al_2SiO_5 polymorphs. American Mineralogist, 76, 677–680.

Burt, D.M. (1989) Vector representation of tourmaline compositions. American Mineralogist, 74, 826–839.

Cameron, W.E. (1977) Mullite: a substituted alumina. American Mineralogist, 62, 747–753.

Carson, C.J., Hand, M., and Dirks, P.H.G.M. (1995) Stable coexistence of grandidierite and kornerupine during medium pressure granulite facies metamorphism. Mineralogical Magazine, 59, 327–339.

Carson, C.J., Powell, R., Wilson, C.J.L., and Dirks, P.H.G.M. (1997) Partial melting during tectonic exhumation of a granulite terrane: an example from the Larsemann Hills, East Antarctica. Journal of Metamorphic Geology, 15, 105–126.

Chorlton, L.B. (1973) The effect of boron on phase relations in the granite-water system, 95 p. M.S. thesis, McGill University, Montreal, Canada.

Chorlton, L.B. and Martin, R.F. (1978) The effect of boron on the granite solidus. Canadian Mineralogist, 16, 239–244.

Cooper, M. (1997) The crystal chemistry of kornerupine, 199 p. M.S. thesis, University of Manitoba, Winnipeg, Canada.

Deer, W.A., Howie, R.A., and Zussman, J. (1982) Sillimanite, Mullite. In Rock-forming minerals, vol. 1A: Orthosilicates (2nd edition), p. 719–758. Longmans, London.

Dietzel, A. and Scholze, H. (1955) Untersuchungen im System B_2O_3-Al_2O_3-SiO_2. Glastechnische Berichte, 28, 47–51.

Dingwell, D.B., Pichavant, M., and Holtz, F. (1996) Experimental studies of boron in granitic melts. In Mineralogical Society of America Reviews in Mineralogy, 33, 331–385.

Dirks, P.H.G.M., Carson, C.J., and Wilson, C.J.L. (1993) The deformational history of the Larsemann Hills, Prydz Bay: the importance of the Pan-African (500 Ma) in East Antarctica. Antarctic Science 5(2), 179–192.

Evers, T.J.J.M. and Wevers, J.M.A. (1984) The composition and related optical axial angle of sillimanites sampled from the high-grade metamorphic Precambrian of Rogaland, SW Norway. Neues Jahrbuch für Mineralogie Monatshefte, 1984(2), 49–60.

Gelsdorf, G., Müller-Hesse, H., and Schwiete, H.-E. (1958) Einlagerungsversuche an synthetischem Mullit und Substitutionsversuche mit Galliumoxyd und Germaniumdioxyd. Teil II. Archiv für das Eisenhüttenwesen, 29(8), 513–519.

Gielisse, P.J.M. (1961) Investigation of phase equilibria in the system alumina-boron oxide-silica, 90 p. Ph.D. thesis, Ohio State University, Columbus, Ohio.

Gielisse, P.J.M. and Foster, W.R. (1961) Research on phase equilibria be-

tween boron oxides and refractory oxides, including silicon and aluminum oxides, 10 p. Quarterly Progress Report by the Ohio State University Research Foundation.

———(1962) The system Al_2O_3-B_2O_3. Nature, 195, 69–70.

Grew, E.S. (1996) Borosilicates (exclusive of tourmaline) and boron in rock-forming minerals in metamorphic environments. In Mineralogical Society of America Reviews in Mineralogy, 33, 387–502.

Grew, E.S., Cooper, M.A., and Hawthorne, F.C. (1996) Prismatine: revalidation for boron-rich compositions of the kornerupine group. Mineralogical Magazine, 60, 483–491.

Grew, E.S., Yates, M.G., Huijsmans, J.P.P., McGee, J.J., Shearer, C.K., Wiedenbeck, M., and Rouse, R.C. (1998) Werdingite, a borosilicate new to pegmatites. Canadian Mineralogist (in press).

Henry, D.J. and Dutrow, B.L. (1996) Metamorphic tourmaline and its petrologic applications. In Mineralogical Society of America Reviews in Mineralogy, 33, 503–557.

Hervig, R.L. (1996) Analyses of geological materials for boron by secondary ion mass spectrometry. In Mineralogical Society of America Reviews in Mineralogy, 33, 789–803.

Huijsmans, J.P.P. (1981) A grandidierite-bearing pegmatite from the Almgjotheii, Rogaland, SW Norway, 38 p. M.S. thesis (Petrology) Institute of Earth Sciences, State University of Utrecht, The Netherlands (in Dutch).

Huijsmans, J.P.P., Kabel, A.B.E.T., and Steenstra, S.E. (1981) On the structure of a high-grade metamorphic Precambrian terrain in Rogaland, south Norway. Norsk Geologisk Tidsskrift, 61, 183–192.

Huijsmans, J.P.P., Barton, M., and van Bergen, M.J. (1982) A pegmatite containing Fe-rich grandidierite, Ti-rich dumortierite and tourmaline from the Precambrian, high-grade metamorphic complex of Rogaland, S.W. Norway. Neues Jahrbuch für Mineralogie Abhandlungen, 143, 249–261.

Ihara, M., Imai, K., Fukunaga, J., and Yoshida, N. (1980) Crystal structure of boroaluminate, $9Al_2O_3 2B_2O_3$. Yogyo-Kyokai-Shi 88(2), 77–84 (in Japanese with English abstract).

Jansen, J.B.H., Blok, R.J.P., Bos, A., and Scheelings, M. (1985) Geothermometry and geobarometry in Rogaland and preliminary results from the Bamble area, S Norway. In A.C. Tobi and J.L.R. Touret, Eds., The Deep Proterozoic Crust in the North Atlantic Provinces, NATO ASI Series C, vol. 158, p. 499–516. Reidel, Dordrecht, The Netherlands.

Jolliff, B.L., Papike, J.J., and Shearer, C.K. (1986) Tourmaline as a recorder of pegmatite evolution: Bob Ingersoll pegmatite, Black Hills, South Dakota. American Mineralogist, 71, 472–500.

Kerrick, D.M. (1972) Experimental determination of muscovite + quartz stability with $P_{H_2O} < P_{total}$. American Journal of Science, 272, 946–958.

———(1990) The Al_2SiO_5 polymorphs, 406 p. Mineralogical Society of America Reviews in Mineralogy, 22.

Kim, K.H. (1961) Phase equilibria in the system Li_2O-B_2O_3-Al_2O_3-SiO_2 and some of its subsidiary systems, 186 p. Ph.D. thesis, Pennsylvania State University, University Park, Pennsylvania.

Kobayashi, H., Toda, K., Kohno, H., Arai, T., and Wilson, R. (1995) The study of some peculiar phenomena in ultra-soft X-ray measurements using synthetic multilayer crystals. Advances in X-ray Analysis, 38, 307–312.

Kretz, R. (1983) Symbols for rock-forming minerals. American Mineralogist, 68, 277–279.

Letort, Y. (1952) Contribution à l'étude de la synthèse de la mullite. Transactions of the International Ceramic Congress, p. 19–32.

London, D. and Manning, D.A.C. (1995) Chemical variation and significance of tourmaline from southwest England. Economic Geology, 90, 495–519.

Maijer, C. (1987) The metamorphic envelope of the Rogaland intrusive complex. In C. Maijer and P. Padget, Eds., The Geology of Southernmost Norway: An excursion guide. Norges Geologiske Undersøkelse Special Publication no. 1, 68–73.

Maijer, C., Andriessen, P.A.M., Hebeda, E.H., Jansen, J.B.H., and Verschure, R.H. (1981) Osumilite, an approximately 970 Ma old high-temperature index mineral of the granulite-facies metamorphism in Rogaland, SW Norway. Geologie en Mijnbouw, 60, 267–272.

Mandarino, J.A. (1981) The Gladstone-Dale relationship: Part IV. The compatibility concept and its application. Canadian Mineralogist, 19, 441–450.

Mazza, D., Vallino, M., and Busca, G. (1992) Mullite-type structures in the systems Al_2O_3-Me_2O (Me = Na, K) and Al_2O_3-B_2O_3. Journal of the American Ceramic Society, 75, 1929–1934.

McGee, J.J. and Anovitz, L.M. (1996) Electron probe microanalysis of geologic materials for boron. In Mineralogical Society of America Reviews in Mineralogy, 33, 771–788.

Moore, J.M., Waters, D.J., and Niven, M.L. (1990) Werdingite, a new borosilicate mineral from the granulite facies of the western Namaqualand metamorphic complex, South Africa. American Mineralogist, 75, 415–420.

Novoselova, L.N. and Sosedko, T.A. (1991) Authigenic tourmaline from carbonate rocks of the Batenev Ridge (Altay-Sayan fold region). Zapiski Vsesoyuznogo Mineralogicheskogo Obshchestva, 120(1), 79–83 (in Russian).

Pichavant, M. (1979) Étude expérimentale à haute température et 1 kbar du rôle du bore dans quelques systèmes silicatés. Intérêt pétrologique et métallogénique, 153 p. Thèse de Spécialité, INPL, Nancy.

———(1981) An experimental study of the effect of boron on a water saturated haplogranite at 1 kbar vapour pressure. Contributions to Mineralogy and Petrology, 76, 430–439.

Ren, L. and Liu, X. (1994) Tourmaline and its relationship with metamorphism, Zhongshan Station, Antarctica. Yanshi Kuangwuxue Zashi (Acta Petrologica et Mineralogica), 13(2), 169–174 (in Chinese with English abstract and Chemical Abstracts 122:35290j)

Ren, L., Zhao, Y., Liu, X., and Chen, T. (1992) Re-examination of the metamorphic evolution of the Larsemann Hills, East Antarctica. In Y. Yoshida, K. Kaminuma, and K. Shiraishi, Eds., Recent Progress in Antarctic Earth Science, p. 145–153. Terrapub, Tokyo.

Rosenberg, P.E., Foit, F.F., Jr., and Ekambaram, V. (1986) Synthesis and characterization of tourmaline in the system Na_2O-Al_2O_3-SiO_2-B_2O_3-H_2O. American Mineralogist, 71, 971–976.

Scholze, H. (1956) Über Aluminiumborate. Zeitschrifte für Anorganische Allgemeine Chemie, 284, 272–277.

Sokolova, Y.V., Azizov, A.V., Simonov, M.A., Leonyuk, N.I., and Belov, N.V. (1978) Crystal structure of synthetic ortho-3-borate $Al_5(BO_3)O_6$. Doklady Akademii Nauk SSSR, 243, 655–658 (in Russian).

Sperlich, R., Gieré, R., and Frey, M. (1996) Evolution of compositional polarity and zoning in tourmaline during prograde metamorphism of sedimentary rocks in the Swiss Central Alps. American Mineralogist, 81, 1222–1236.

Stüwe, K. and Powell, R. (1989a) Low-pressure granulite facies metamorphism in the Larsemann Hills area, East Antarctica; petrology and tectonic implications for the evolution of the Prydz Bay area. Journal of Metamorphic Geology, 7, 465–483.

———(1989b) Metamorphic segregations associated with garnet and orthopyroxene porphyroblast growth: two examples from the Larsemann Hills, East Antarctica. Contributions to Mineralogy and Petrology, 103, 523–530.

Stüwe, K., Braun, H.-M., and Peer, H. (1989) Geology and structure of the Larsemann Hills area, Prydz Bay, East Antarctica. Australian Journal of Earth Sciences, 36, 219–241.

Su, S.-C. (1993) Determination of refractive index of solids by dispersion staining method—an analytical approach. In C.L. Rieder, Ed., Proceedings of 51st Annual Meeting of the Microscopy Society of America, 456–457.

Thompson, J.B., Jr. (1982) Composition space: An algebraic and geometric approach. In Mineralogical Society of America Reviews in Mineralogy, 10, 1–31.

Tobi, A.C., Hermans, G.A.E.M., Maijer, C., and Jansen, J.B.H. (1985) Metamorphic zoning in the high-grade Proterozoic of Rogaland-Vest Agder, SW Norway. In A.C. Tobi and J.L.R. Touret, Eds., The deep Proterozoic crust in the North Atlantic Provinces, NATO ASI Series C, vol. 158, p. 477–497. Reidel, Dordrecht, The Netherlands.

Werding, G. and Schreyer, W. (1984) Alkali-free tourmaline in the system

MgO-Al_2O_3-B_2O_3-SiO_2-H_2O. Geochimica et Cosmochimica Acta, 48, 1331–1344.

———(1992) Synthesis and stability of werdingite, a new phase in the system MgO-Al_2O_3-B_2O_3-SiO_2 (MABS), and another new phase in the ABS-system. European Journal of Mineralogy, 4, 193–207.

———(1996) Experimental studies on borosilicates and selected borates. In Mineralogical Society of America Reviews in Mineralogy, 33, 117–163.

Wilmart, E. and Duchesne, J.-C. (1987) Geothermobarometry of igneous and metamorphic rocks around the Åna-Sira anorthosite massif: Implications for the depth of emplacement of the South Norwegian anorthosites. Norsk Geologisk Tiddskrift, 67, 185–196.

Wolf, M.B. and London, D. (1997) Boron in granitic magmas: Stability of tourmaline in equilibrium with biotite and cordierite. Contributions to Mineralogy and Petrology, 130, 12–30.

Manuscript received March 14, 1997
Manuscript accepted January 8, 1998
Paper handled by Lee A. Groat